JTTEE5 3:389-397

Interaction of Particles with Carrier Gas in HVOF Spraying Systems

E. Kadyrov, Y. Evdokimenko, V. Kisel, V. Kadyrov, and F. Worzala

Several designs of high-velocity oxygen fuel (HVOF) thermal spray systems have been created during the last decade. The most advanced systems are now producing coatings comparable in quality to detonation (D-gun) coatings. This paper presents numerical analysis of the interaction of dispersive particles with the carrying gas flow for three different HVOF systems, along with a method to calculate the parameters of sprayed particles that highlights the advantages and limitations of each design. The method includes gas dynamical calculations of the gas flow in an accelerating channel and calculations of the injected particle motion and thermal state (temperature and melted mass fraction). The calculations were performed for particles of tungsten carbide, aluminum oxide, and zirconium oxide with size distributions of 10 to 80 μm. Two conventional types of HVOF systems were considered: those with a supersonic accelerating channel and those with a subsonic accelerating channel (without a de Laval nozzle). A novel design is proposed that contains a combined gas dynamical path with functionally separated regions of heating and acceleration. The regularities and distinctions in the behavior of the metallic and ceramic oxide particles are discussed for different jet configurations. The results obtained indicate that it is possible to significantly affect particle parameters by using the new configuration solutions without creating construction complications.

1. Introduction

MANY investigations have focused on the high-velocity oxygen fuel (HVOF) thermal spray process. However, a detailed understanding of the gas dynamics of the process—that is, the interaction between the injected particle and the gas flow in the system and its relation to the final quality of the coating—has not yet been achieved. This paper presents numerical analysis of three different HVOF systems and discusses the effects of design variations on the final parameters of the particles. Results are presented for three widely used thermal spray materials: tungsten carbide, aluminum oxide, and zirconium oxide with size distributions of 10 to 80 μm. The paper is organized as follows. Section 2 classifies conventional designs of HVOF jets and discusses some optimal parameters of their operation. Section 3 describes the governing equations and the computational procedures used to determine gas flow and particle parameters. The dimensionless energy parameter K_e is introduced, which incorporates both the kinetic and thermal energies of the particles and which is proposed as a parameter of coating quality control. In section 4, the described method is applied to investigate the effect of pressure and temperature in the combustion chamber on the output particle parameters. Section 5 describes a proposed option for the enhancement of the gas dynamical path of an HVOF jet. Section 6 presents the results of calculations of the velocity, thermal state, and energy parameter for three HVOF designs with different configurations of the gas dynamical path. Better understanding of the gas dynamics of the complex HVOF spraying process and interactions in the two-phase flow allows different HVOF design schemes to be evaluated.

Keywords de Laval nozzle, gas dynamics, high-velocity oxygen fuel, particle kinetic energy, particle temperature

E. Kadyrov and **F. Worzala,** Materials Science Program, University of Wisconsin—Madison, Madison, WI 53706, USA; **Y. Evdokimenko, V. Kisel,** and **V. Kadyrov,** Research Institute of Materials Science, Ukrainian Academy of Sciences, Kiev 252142, Ukraine.

2. Background

2.1 *HVOF System Designs*

The HVOF powder spraying method involves continuous burning of the oxygen-fuel mixture as powder particles are injected into the hot stream of accelerating gas. This can be accomplished using several possible design solutions. These designs differ in jet geometry (size and configuration of different parts), cooling system, method of powder and fuel injection, fuel selection, and so on. This paper investigates the influence of jet geometry on the parameters of gas flow and particle states. The terminology presented in Ref 1 will be followed. There are throat combustion burners (Ref 2), which have a reduced burner chamber diameter, and chamber combustion burners (Ref 3), which contain a larger-diameter combustion chamber. According to Ref 1, there are water-cooled throat combustion burners with axial injection; air-cooled throat combustion burners with axial injection; and water-cooled chamber combustion burners with axial injection, right-angle axial injection, and radial throat injection. However, one important distinction exists in the configuration of the gas path in all of these types of apparatus. One group of equipment (for example, the JP-5000 HP/HVOF) utilizes a de Laval nozzle (a narrowing of the throat inside the accelerating barrel) (Ref 4, 5) to create supersonic flow inside the apparatus; the other group does not contain such a nozzle. In the second case, the exit cross section of the barrel plays the role of a de Laval nozzle; and supersonic speed is reached after the stream leaves the apparatus, whereas particle acceleration occurs inside the apparatus in subsonic flow. An example of this configuration is found in the apparatus of the JetKote (Ref 6) system. Mechanisms of particle heating and acceleration differ significantly for these two groups of equipment. In the first

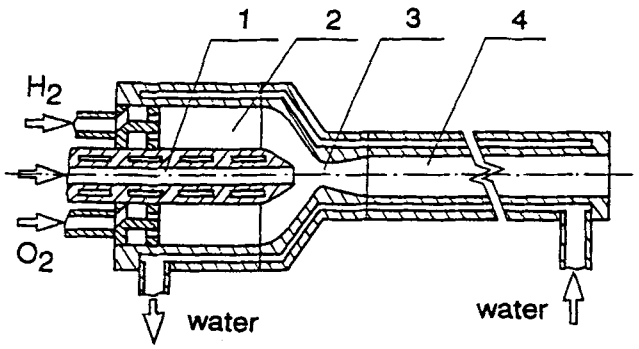

Fig. 1 Gas dynamical path of STREAM HVOF spraying apparatus. 1, powder feeding duct; 2, combustion chamber; 3, supersonic de Laval nozzle; 4, accelerating channel

group, acceleration occurs over a longer supersonic interval, and thus the magnitude of the final particle velocity is higher, making the time spent by the particle inside the apparatus shorter and correspondingly lowering the final particle temperature. The second type of equipment produces lower magnitudes of final velocity and higher final particle temperatures. These equipment differences will become more apparent in the subsequent discussion. Obviously, both kinetic energy and thermal energy are important parameters for the sprayed powders. It is not quite clear which type of design will produce coatings of higher quality.

Figure 1 shows the gas path of supersonic flame-spraying equipment (known as STREAM) developed by the authors. This is a water-cooled jet with axial powder injection and a de Laval nozzle—a typical configuration for torches utilizing the HVOF process. It consists of a combustion chamber, in which the flammable mixture is injected and burned; a supersonic de Laval nozzle; and a cylindrical accelerating channel, in which the speed of the gas flow is from M1.3 to M2.0. The accelerating channel represents the transonic nozzle if the supersonic nozzle is absent; that is, sonic speed is reached by the burned products at the exit cross section, while inside the chamber the gas flow has the speed M0.85 to M1.0. This scheme is utilized, for instance, in the JetKote II (Ref 7) apparatus. In both cases, the feedstock is injected axially or radially into the narrow area inside the accelerating channel, and its acceleration and heating occur in the high-speed stream of gas. Attempts to inject the powder directly into the combustion chamber failed because of the significant reduction in reliability and lifetime of the apparatus.

2.2 *Operational Conditions and Particle Temperature during the HVOF Process*

The high speed of the gas stream in the accelerating channel provides effective acceleration of the relatively light particles of sprayed powders and at the same time prevents the particles from completely utilizing the energetic resource of the burning flammable mixture for heating. This happens for two reasons. First, the high velocity gained by the powder particles in the first moments of their acceleration in the channel does not allow sufficient time in the high-temperature region for effective heating. Calculation shows that in the first 10% of the accelerating channel length, the particles are accelerated to 33% of their final velocity (Ref 8), and the average speed of the particles inside the channel is more than 75% of their velocity at the channel exit. For an HVOF system with an internal de Laval nozzle, the average final particle speed is 600 m/s and the total length of the accelerating channel typically does not exceed 20 times the channel diameter (160 mm at the diameter of critical cross section d_c = 8 mm); therefore, the effective time spent by the particles inside the accelerating channel is 0.4 ms. During this time, the ceramic oxide powders do not reach the temperatures needed to produce a quality coating. Second, the temperature in the subsonic and supersonic part of the stream is significantly less than the temperature in the combustion chamber. For example, the temperature in the combustion chamber at a stoichiometric ratio of oxygen and hydrogen and a pressure of 0.5 MPa is about 3240 K. The temperature in the stream is 3000 K at M1.0 and 2500 K at M1.9. At the average speed of the gas stream (2000 m/s), the thermodynamical temperature of the gas is 2700 K. The thermal state of the particle during the heating process in a medium with a temperature T_f is characterized by its dimensionless temperature θ, which is a monotonically increasing function f of the Fourier (Fo) and Biot (Bi) numbers of the particle (Ref 9). For average particle temperature T_p:

$$\theta = \frac{T_p - T_0}{T_f - T_0} = f(Fo,Bi) \qquad \text{(Eq 1)}$$

with:

$$Fo = \frac{a_p \tau}{d_p^2}$$

$$Bi = \frac{\alpha d_p}{\lambda_p} = Nu \frac{\lambda_f}{\lambda_p}$$

$$a_p = \frac{\lambda_p}{c_p \rho_p}$$

where d_p is the diameter of the particle; τ is heating time; λ_p is the heat conduction of the particle; λ_f is the heat conduction of the gas phase; α is the coefficient of heat exchange between particle and gas; Nu is the Nusselt number, which defines heat exchange between the body and the surrounding gas; c_p is the specific heat of the particle; ρ_p is particle density; and T_0 is the initial temperature of the particle. For the flow around the spherical particle:

$$Nu = 2 + 0.6Re^{0.5}Pr^{0.33} \qquad \text{(Eq 2)}$$

where Re and Pr are the Reynolds and Prandtl numbers (Ref 10), respectively. The Prandtl number for the burning of carbon-hydrogen fuels in oxygen can be assumed to be constant: $Pr^{0.33}$ = 0.84. Thus, the thermal state of the particle is defined by the time τ spent inside the flow, the gas temperature T_f, and the Reynolds number:

$$Re = \frac{u \rho_f d_p}{\mu_f} \qquad \text{(Eq 3)}$$

where u is a relative speed of particle motion, ρ_f is gas density, and μ_f is gas viscosity. An increase in the Fourier and Biot numbers will result in increased particle temperature. However, this increase is limited because the accelerating channel has a finite length, and the temperature and pressure in the combustion chamber are also limited. The temperature of the burned products in the combustion chamber when hydrogen is the fuel gas and oxygen is the oxidizer is 3240 K at a pressure of 0.5 MPa and 3330 K at a pressure of 1 MPa. A higher temperature is achieved (greater than 3400 K) when an oxygen-acetylene mixture is used; however, this mixture is hazardous.

The effect of pressure in the combustion chamber on particle temperature has several consequences. A pressure increase is accompanied by an increase in temperature in the combustion chamber. On the other hand, the pressure increase intensifies particle acceleration, lessening the time spent inside the accelerating channel. Calculations show that a pressure increase in an apparatus with a subsonic accelerating chamber will decrease the particle temperature. The pressure effect will be discussed in the next section. Calculations and operating experience of the STREAM equipment show that a pressure increase above 1.0 to 1.2 MPa in industrial conditions is economically inefficient. The length of the accelerating channel is limited by the conditions necessary for the existence of supersonic flow and, for a gas speed of M2, cannot exceed 50 times the accelerating channel diameter. In practice, this length is typically 20 to 25 times the accelerating channel diameter (i.e., up to 200 mm). Use of longer channels (up to 35 times the accelerating channel diameter) provides no noticeable increase in the particle parameters; however, reducing the total pressure in the flow reduces thermal effects on the substrate.

Therefore, a supersonic torch utilizing gaseous oxygen and hydrogen at 1 MPa pressure for a 6 mm diam nozzle and 350 mm long accelerating channel can be considered optimal for HVOF industrial applications. These parameters were used in the numerical analysis of several designs.

3. Governing Equations and Computational Technique

3.1 *Kinematic Equations*

The method includes calculations of the gas flow in the accelerating channel for different design parameters and calculations of the particle motion and its thermal state. During the spraying process, the typical value of volume concentration of particles is $\beta_p = 10^{-5}$, which allows one to ignore the effects of particles on the flow parameters that are dominated by the effects of wall friction and cooling at the surface of the accelerating chamber. Interparticle interaction, which becomes important at concentrations of $\beta_p > 5 \times 10^{-3}$, also can be neglected. Under these assumptions, the problem is solvable by means of a one-particle approximation. The calculation is performed in a quasi-one-dimensional case (Ref 11) taking into account flow friction at the walls of the accelerating channel and neglecting flow cooling in the vicinity of the walls. A spherical shape of the feedstock is assumed. The equation of motion for one spherical particle accelerating in a carrying flow is (Ref 10):

$$m_p \frac{dV}{dt} = c_\mu \psi_\mu \frac{\rho_f (W - V)^2}{2} \frac{\pi d_p^2}{4} \quad \text{(Eq 4)}$$

where m_p is particle mass, V is particle speed, W is velocity of the gas flow, c_μ is a coefficient of aerodynamic resistance of the hard sphere in the noncompressible fluid, and ψ_μ is a coefficient that accounts for gas compressibility at M = 0.2 to 1.0 and Re = 200 to 1000. After transformations, Eq 4 is reduced to:

$$\frac{V}{(W - V)^2} dV = \frac{3}{4} \frac{c_\mu \psi_\mu \rho_f}{d_p \rho_p} dx \quad \text{(Eq 5)}$$

where x is the coordinate along the accelerating channel. Solution of this equation is the expression:

$$\frac{W}{W - V} + \ln(W - V) = \frac{W}{(W - V_0)} + \ln(W - V_0) + \frac{3}{4} \frac{c_\mu \psi_\mu \rho_f x}{d_p \rho_p} \quad \text{(Eq 6)}$$

which allows numerical calculation of particle speed at the exit of the accelerating channel. Final velocity as a function of particle density, diameter, initial speed V_0, and other parameters is iteratively calculated from the initial cross section of the accelerating channel to its exit cross section. Coefficients c_μ and ψ_μ are functions of the Reynolds and mach numbers and are given by the expression (Ref 12):

$$c_\mu = \frac{21.1}{\mathrm{Re}} + \frac{6.3}{\sqrt{\mathrm{Re}}} + 0.25 \quad \text{(Eq 7)}$$

$$\psi_\mu = (1 + 1.2\mathrm{M}c_\mu)^{-0.5} \cdot (1 - 0.445\mathrm{M} + 4.84\mathrm{M}^2 - 9.73\mathrm{M}^3 + 6.94\mathrm{M}^4) \quad \text{(Eq 8)}$$

3.2 *Calculation of the Thermal State*

Calculation of the thermal state for ceramic particles is a more complicated problem. The typical equation of heat balance,

$$m_p c_p(T) dT = \alpha (T_f - T) S_p d\tau \quad \text{(Eq 9)}$$

where $c_p(T)$ is particle specific heat and S_p is particle surface area, gives relatively valid results for heating of metallic particles (Ref 13). This approach was used to calculate the thermal state of tungsten carbide particles. The coefficient of heat exchange, α, on the particle can be found using Eq 1 with the following expressions for Nu and Pr:

$$\mathrm{Nu} = \frac{\alpha d_c}{\lambda_f}, \quad \mathrm{Pr} = \frac{c_{pf} \mu_f}{\lambda_f} \quad \text{(Eq 10)}$$

where c_{pf}, λ_f, and μ_f are the specific heat, heat conduction, and viscosity, respectively, of the gas phase. Solution of the heat-balance equation under the assumption of constant specific heat takes the form:

$$T = T_f - (T_f - T_0) \exp\left(-\frac{6\alpha\tau}{c_p \rho_p d_p}\right) \quad \text{(Eq 11)}$$

where T_f is the average gas temperature in the accelerating channel and T_0 is initial particle temperature. Equation 11 allows iterative calculation of the temperature along the length of the accelerating channel. The equation of heat balance during the melting stage is:

$$Q_m m\, d\eta = \alpha(T_f - T_m) S d\tau \quad \text{(Eq 12)}$$

where η is the fraction of melted mass, Q_m is the melting specific heat, and T_m is the melting point of the material. Correspondingly, the fraction of melted mass is related to melting time $d\tau$ by:

$$d\eta = \frac{6\alpha(T_f - T_m)d\tau}{Q_m \rho_c d_c} \quad \text{(Eq 13)}$$

Equations 1 to 13, by utilizing known distributions of gas velocity, gas density, and gas temperature along the accelerating channel, allow calculation of velocity, temperature, and fraction of melted mass for the sprayed particle. For ceramic particles that have low heat conduction (coefficient of heat conduction for oxide ceramics is typically two orders of magnitude lower than for metals), this approach is not acceptable since it assumes that the temperature inside the particle is uniform. For ceramic particles at conditions similar to HVOF spraying conditions, the surface temperature can be twice as high as the temperature at the center, resulting in higher (about 1.5 times) values of average particle temperature. Thus, for particles of low heat conduction, one needs to calculate the temperature field inside the particle and find the average temperature. The approach in this calculation is based on utilizing classical solutions for the temperature field inside a spherical body of radius R having a constant initial temperature T_0 and placed into a medium of constant temperature $T_{fe} > T_0$. The standard solution for the temperature at a position with radius r takes the form (Ref 9):

$$\theta_r = 1 - \sum_{n=1}^{n=\infty} A_n \frac{R \sin\left(\mu_n \frac{r}{R}\right)}{r\mu_n} \exp(-\mu_n^2 \mathrm{Fo}) \quad \text{(Eq 14)}$$

and coefficients A_n are given by:

$$A_n = (-1)^{n+1} \frac{2Bi\sqrt{\mu_n^2 + (Bi-1)^2}}{\mu_n^2 + Bi^2 - Bi} \quad \text{(Eq 15)}$$

where μ_n are the roots of the characteristic equation:

$$tg\mu = -\frac{\mu}{Bi - 1} \quad \text{(Eq 16)}$$

The solution for the average temperature θ is:

$$\theta = 1 - \sum_{n=1}^{n=\infty} c_n \exp(-\mu_n^2 \mathrm{Fo}) \quad \text{(Eq 17)}$$

with the coefficients:

$$c_n = \frac{6Bi^2}{\mu_n^2(\mu_n^2 + Bi^2 - Bi)} \quad \text{(Eq 18)}$$

This approach was used to evaluate the temperature field inside the ceramic oxide particles and to find their average temperature. Summations in Eq 14, 15, 17, and 18 were truncated to n values of less than seven.

Complicated patterns exist in the supersonic stream after it leaves the de Laval nozzle (Ref 10, 11). The rapid change in both flow direction and pressure when leaving the divergent section of the nozzle to the barrel sets up a Prandt-Meyer flow in the barrel consisting of weak expansion and compression waves. The presence of oblique reflected waves sets up a pattern known as "shock diamonds." Our analysis assumes that the flow is adiabatic and quasi-one-dimensional, and thus neglects transverse effects arising from the interference of oblique waves. To model the real gas flow, an equivalent gas flow is introduced having constant temperature T_{fe} and constant coefficient of heat exchange with the particle α_e. This assumption is based on the fact that temperature and coefficient of heat exchange in the flow are changing in a limited range (about 15%). Equivalent temperature T_{fe} and equivalent coefficient of heat exchange are calculated by averaging the distributions of real temperature and real heat-exchange coefficient over the time spent by the particle inside the accelerating channel. Particle heat-exchange coefficient, temperature, and velocity distributions in the gas flow were calculated for given design parameters using commercial software developed at the Institute of Aviation (Moscow). The solutions of Eq 1 to 9 along with Eq 13 to 18 were incorporated in a computer program that allowed calculation of particle velocity and thermal state (with knowledge of the powder material, size, and equivalent flow parameters). Results are presented in subsequent sections.

3.3 *Particle Energy Parameter*

Part of the particle kinetic energy transforms into thermal energy during collision with the substrate. Thus, both temperature and kinetic energy of the powder are important parameters for quality coating formation. Therefore, an energy parameter K_e, which characterizes both particle temperature and kinetic energy and which also directly affects coating quality, is chosen to be the ratio of the sum of specific enthalpy $H(T_p)$ and specific kinetic energy to the enthalpy of the completely melted particle at melting point T_m:

$$K_e = \frac{H(T_p) + 0.5 V_p^2}{\int_{T_0}^{T_m} C_p(T)dT + Q_m} \quad \text{(Eq 19)}$$

where Q_m is the melting specific heat. When the particle reaches its melting point and some fraction η of its mass is melted, the specific enthalpy is:

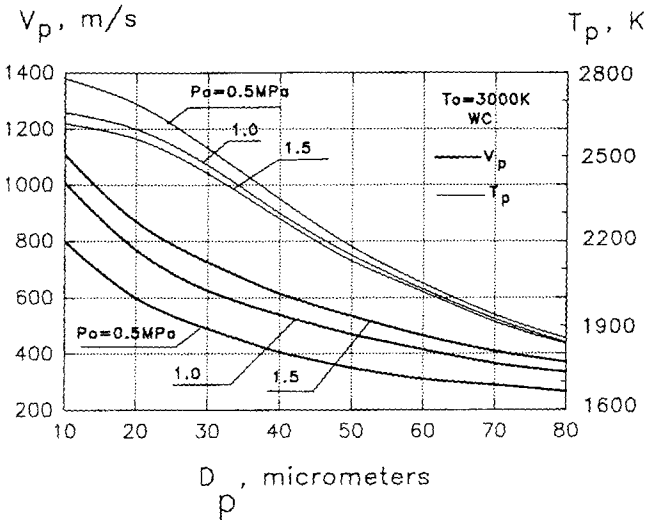

Fig. 2 Effect of pressure in the combustion chamber on the velocity and temperature of tungsten carbide particles as a function of particle size for $T_0 = 3000$ K

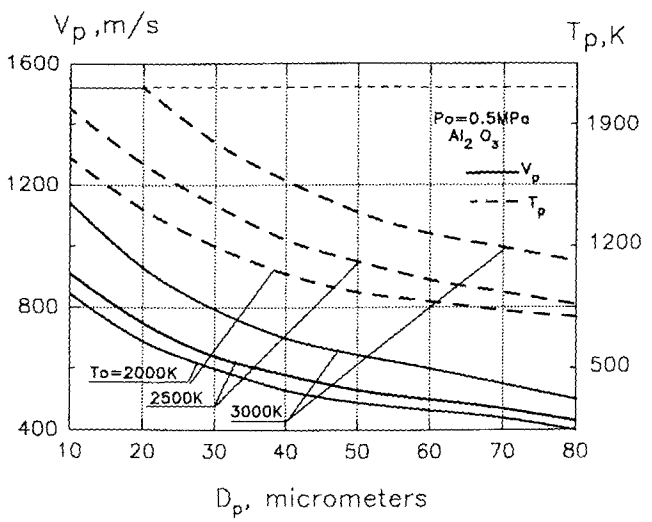

Fig. 3 Effect of temperature in the combustion chamber on the velocity and temperature of aluminum oxide particles as a function of particle size for $P_0 = 0.5$ MPa

$$H(T_m) = \int_{T_0}^{T_m} C_p(T)dT + \eta Q_m \qquad \text{(Eq 20)}$$

The kinetic parameter K_e characterizes the possibility of particle melting during its collision with the substrate under the condition that all kinetic energy is transformed into thermal energy and is absorbed by the particle. Then the minimum value of the kinetic parameter

$$K_{e\,min} = \frac{\int_{T_0}^{T_m} C_p(T)dT}{\int_{T_0}^{T_m} C_p(T)dT + Q_m} \qquad \text{(Eq 21)}$$

corresponds to the attainment of melting point by the particle, and a value $K_e = 1$ corresponds to complete melting of the particle (for Al_2O_3, $K_{e\,min} = 0.71$; for ZrO_2, $K_{e\,min} = 0.67$). Correspondingly, in the region $K_{e\,min} < K_e < 1$, the fraction of the melted mass in the particle at the collision is:

$$\eta = \frac{K_e - K_{e\,min}}{1 - K_{e\,min}} \qquad \text{(Eq 22)}$$

For the formation of quality metallurgical bonding of the coating to the substrate, it is necessary to overheat (Ref 13) the sprayed particles by a factor of 0.1 to 0.3 T_m. In addition, the kinetic energy does not completely transform into thermal heat during collision. Thus, the condition for the formation of a high-quality coating is $K_e > 1$. This approach allows incorporation of both the kinetic energy and the thermal energy of the particle into one dimensionless parameter that quantifies particles output parameters and which can be correlated with coating quality.

4. Effects of Combustion Chamber Pressure and Temperature on Aluminum Oxide and Tungsten Carbide Particle Parameters

This section investigates the effects of combustion chamber pressure and temperature of an HVOF spraying apparatus with a supersonic accelerating channel on the parameters of 10 to 80 μm aluminum oxide and tungsten carbide particles. The parameters were calculated at the exit cross section of the apparatus, which employed a gaseous oxygen-hydrogen fuel mixture at combustion chamber pressures of $P_0 = 0.5$ to 1.5 MPa and temperatures of $T_0 = 2000$ to 3000 K. The supersonic accelerating portion beyond the de Laval nozzle (diameter of 10 mm and length of 200 mm) is considered. The consumption of the combustible mixture was considered to be constant and equal to 15 g/s.

Results are presented in Fig. 2 and 3. Figure 2 illustrates the effect of combustion chamber pressure on velocity and temperature of the tungsten carbide particles for different particle sizes at a chamber temperature of 3000 K. The chamber pressure affects the density of the gas flow and is an important factor in determining the final velocity of the particles. Particle velocity changes in a broad interval depending on particle size. For instance, the velocity of 80 μm particles increases from 260 to 380 m/s as the pressure in the combustion chamber increases from 0.5 to 1.5 MPa, and the corresponding change in the velocity of 10 μm particles is from 800 to 1100 m/s. At the same time, particle temperature is almost completely independent of the pressure in the combustion chamber and is determined by particle size. The temperature of small particles (less than 30 μm) decreases slightly with increasing chamber pressure, which is explained by the thermal relaxation between the particle and the gas phase that occurs as the magnitude of the gas expansion defined by the chamber pressure increases. For example, 10 μm particles have a temperature of 2780 K at a combustion chamber

pressure of 0.5 MPa and a temperature of 2620 K at a pressure of 1.5 MPa. The temperature of 80 μm particles, on the other hand, remains constant at 1860 K as the chamber pressure increases from 0.5 to 1.5 MPa. These results indicate that the optimal range of pressure in the combustion chamber for supersonic gas spraying equipment is 1.0 to 1.5 MPa. A further increase in pressure does not significantly increase particle velocity. Moreover, an increase in pressure increases the dynamic and thermal effects of the stream on the substrate material. Operation of an apparatus at pressures greater than 1.5 MPa also requires equipment modification in the gas supply system.

Figure 3 shows the effect of temperature in the combustion chamber on the parameters of aluminum oxide particles at a constant chamber pressure of 0.5 MPa. A temperature of 3000 K is typical for burning of the hydrogen-containing fuels in pure oxygen, 2500 K for oxygen-enriched air, and 2000 K for air alone. Particle velocity over the entire size range at a combustion chamber temperature of 3000 K is significantly (20 to 25%) higher than at 2000 K, whereas at 2500 and 2000 K the difference in velocities is not significant (approximately 5 to 10%). Therefore, compared with pure air, the use of oxygen-enriched air in the spraying jet offers no significant improvements in particle velocity; however, it allows a slight increase in particle temperature.

Comparison of Fig. 2 and 3 shows that under identical conditions ($P_0 = 0.5$ MPa and $T_0 = 3000$ K) heavy particles of tungsten carbide (density, 15,700 kg/m^3) are accelerated to velocities ranging from 260 m/s for 80 μm particles to 800 m/s for 10 μm particles. These values are slightly lower than the velocities of lighter aluminum oxide particles (density, 3960 kg/m^3), which ranged from 480 to 1150 m/s. At the same time, due to lower specific heat and a higher value of heat conduction, the tungsten carbide particles are heated to much higher temperatures than the aluminum oxide particles (WC, 1860 to 2780 K; Al_2O_3, 1100 to 2300 K). Aluminum oxide particles with a diameter of 20 μm reach their melting point ($T_m = 2300$ K) at an initial combustion chamber temperature of 3000 K, and particles smaller than 10 μm are melted completely. Larger particles of aluminum oxide remain unmelted. This result is supported by the empirical knowledge that oxide ceramics are more difficult to spray than metals or carbides. For example, thermally sprayed oxide coatings characteristically have higher porosity and lower adhesion than carbide coatings. This is related to the fact that although the sprayed particles have relatively high velocities, a large fraction remains unmelted. Modifications of the design configurations allow enhancement of the output particle parameters and improvement of coating quality. The following sections provide analysis of three different HVOF designs and their effects on particle parameters.

5. Proposed Enhancement of Gas Dynamical Path

Results of calculations indicate that particles of aluminum oxide and zirconium oxide larger than 20 to 30 μm sprayed by a typical HVOF system do not reach melting temperature even though a significant fraction of particle kinetic energy is transformed into thermal energy during collision with a target. In such instances, the particle temperature is not sufficiently high to form quality coating. The only way to increase the temperature of the particles when the gas flow temperature is already at a maximum is to increase the residence time of the particles inside the spraying apparatus. This can be achieved either by enlarging the accelerating channel or by decreasing the particle speed inside the channel. One promising way to enhance the performance of HVOF jets—particularly for spraying oxide ceramics and other materials with high specific heat—is to design regions inside the accelerating channel where the speed of the gas flow is significantly lower than sonic speed and is comparable with the gas flow speed in the combustion chamber. In other words, the heating and accelerating processes become functionally separated by special heating regions inside the accelerating channel. One method is to duct into a heating region the gas path that transforms the feedstock. To accomplish this, the burning or flow of hot combustion products with parameters comparable to those of the combustion chamber is organized in the powder feeding duct. Thus, the heating channel represents a separate part of the combustion chamber and supplies heated particles to the accelerating channel, preventing them from scattering in the combustion chamber. Because the velocity of the gas flow in the combustion chamber is low (typically 50 m/s), one might expect a high efficiency of the proposed gas path, since the time spent by the particles inside the 100 mm long heating channel is 2 ms—typically five times longer than traditional HVOF apparatus designs.

6. Results and Discussion

The velocity, thermal state, and energy parameters for 10 to 80 μm particles of aluminum oxide and zirconium oxide were calculated utilizing the described approach. Calculations were performed for the operating parameters of standard HVOF equipment: temperature in the combustion chamber, 3000 K; pressure in the combustion chamber, 1.0 MPa; length of accelerating channel, 350 mm; and consumption of oxygen and hydrogen (at stoichiometric ratio), 15 g/s. Three different configurations of the gas dynamical path were considered (Fig. 4):

- *Configuration 1:* path with supersonic accelerating channel
- *Configuration 2:* path with subsonic accelerating channel
- *Configuration 3:* combined path with functionally separated regions of heating and acceleration

The path of configuration 3 consists of a cylindrical heating channel, cylindrical subsonic accelerating channel, and conical supersonic accelerating channel. The heating channel is 120 mm long with a diameter of 6.5 mm, and it uses one-third of the total gas consumed with a velocity coefficient of $\lambda_1 = 0.2$. The subsonic accelerating channel is 150 mm long with a diameter of 6.5 mm and an entrance speed coefficient of $\lambda_2 = 0.64$. The supersonic accelerating channel is 40 mm long with a diameter increase of 10 mm. Results of calculations are presented in Fig. 5 to 7.

Figures 5(a) and (b) show the velocity of aluminum oxide and zirconium oxide particles, respectively, at the exit cross section of the torch as a function of their size. The velocity of the lighter Al_2O_3 particles is 8 to 12% greater than the velocity of

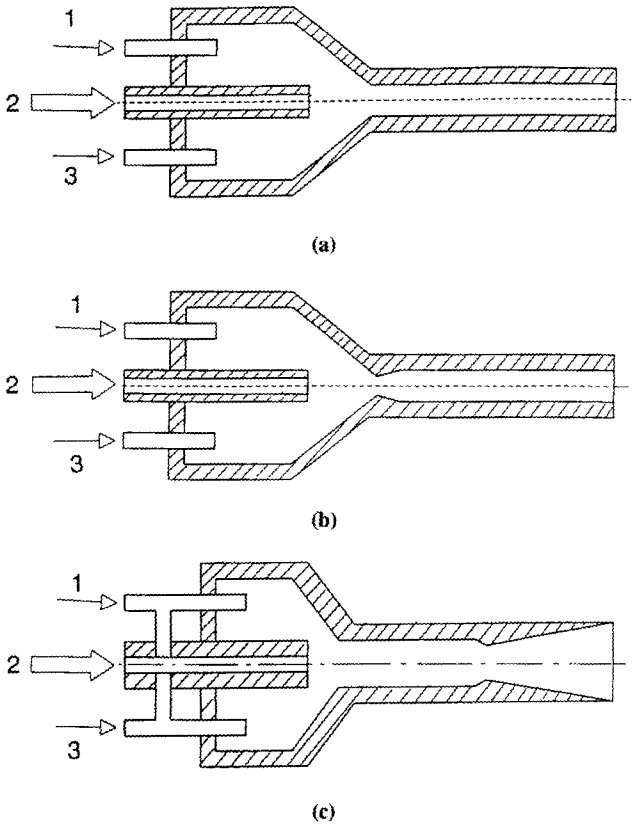

Fig. 4 Schematic diagrams of three HVOF system designs. 1, fuel supply; 2, powder injection; 3, oxygen supply. (a) System with subsonic accelerating channel. (b) System with supersonic accelerating channel. (c) Combined design with additional heating duct

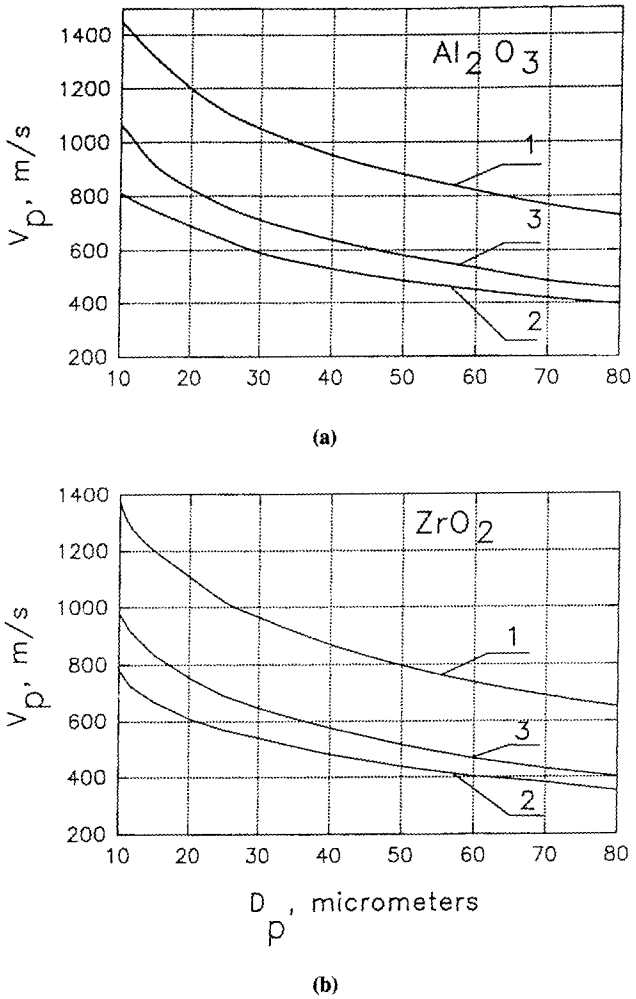

Fig. 5 Exit velocity of (a) Al_2O_3 particles and (b) ZrO_2 particles as a function of particle size for gas path configurations 1 to 3 (see text)

ZrO_2 particles over the entire size range. The acceleration of particles in the supersonic stream is almost twice that of the subsonic stream. The velocity of Al_2O_3 particles reaches 730 to 1410 m/s in the supersonic stream and only 400 to 800 m/s in the subsonic stream. In the combined path the velocity is 12 to 20% greater than in the subsonic path, which is explained by the short path length of supersonic acceleration.

Figures 6(a) and (b) show the final temperature of the Al_2O_3 and ZrO_2 particles, respectively, as a function of their size. Zirconium oxide particles, having less than half the specific heat of Al_2O_3 particles, attain significantly higher temperatures (ZrO_2, 2000 to 2950 K; Al_2O_3, 1500 to 2300 K). Heating is much more effective in the subsonic accelerating channel than in the supersonic channel. In the subsonic channel, Al_2O_3 particles smaller than 30 μm reach their melting point (2300 K), while particles smaller than 20 μm are melted completely, and ZrO_2 particles smaller than 10 μm also reach their melting point (2950 K). In an apparatus with a supersonic channel, aluminum oxide particles up to 12 μm in diameter reach the melting point, and only the melting of very fine particles (smaller than 5 μm) is possible. The temperature of ZrO_2 particles is significantly lower than their melting point in a supersonic channel. The combined path noticeably enhances particle temperature: 40 μm Al_2O_3 particles are heated to the melting point, and particles smaller than 32 μm are melted; ZrO_2 particles smaller than 10 μm are heated to the melting point, and the temperature of large particles (60 to 80 μm) is increased to 2200 K.

Figures 7(a) and (b) show the energy parameters for Al_2O_3 and ZrO_2 particles, respectively, as a function of their size. For aluminum oxide, an HVOF system with a subsonic accelerating channel is energetically more efficient than a system with a supersonic accelerating channel. The subsonic system has an energy parameter for unmelted particles that is 20 to 30% higher than the supersonic system, and for melted particles it is one and a half to two times higher.

As shown in Fig. 7(a), an HVOF system with a supersonic channel does not provide the necessary energy conditions for spraying Al_2O_3 particles larger than 10 μm. Using a jet with a subsonic channel creates favorable conditions for particles up to 20 μm in diameter. The combined path configuration is energetically more efficient than a system with a subsonic channel and can provide the necessary conditions for spraying Al_2O_3 particles up to 30 μm in diameter. Zirconium oxide particles larger than 35 μm exhibit similar tendencies. However, at smaller sizes the supersonic channel becomes more efficient than the sub-

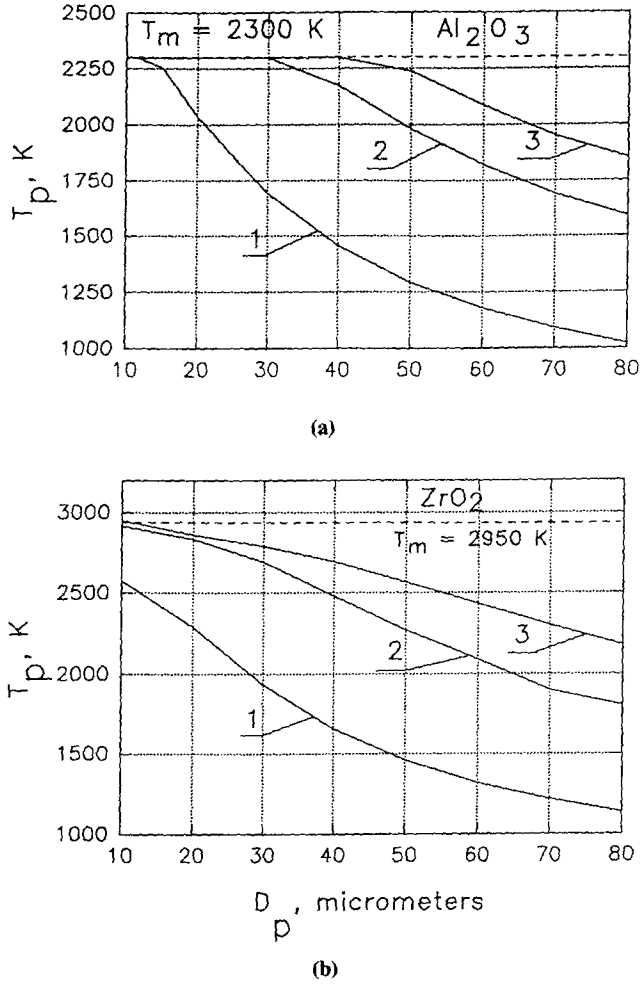

Fig. 6 Temperature of (a) Al_2O_3 particles and (b) ZrO_2 particles as a function of particle size for gas dynamical path configurations 1 to 3

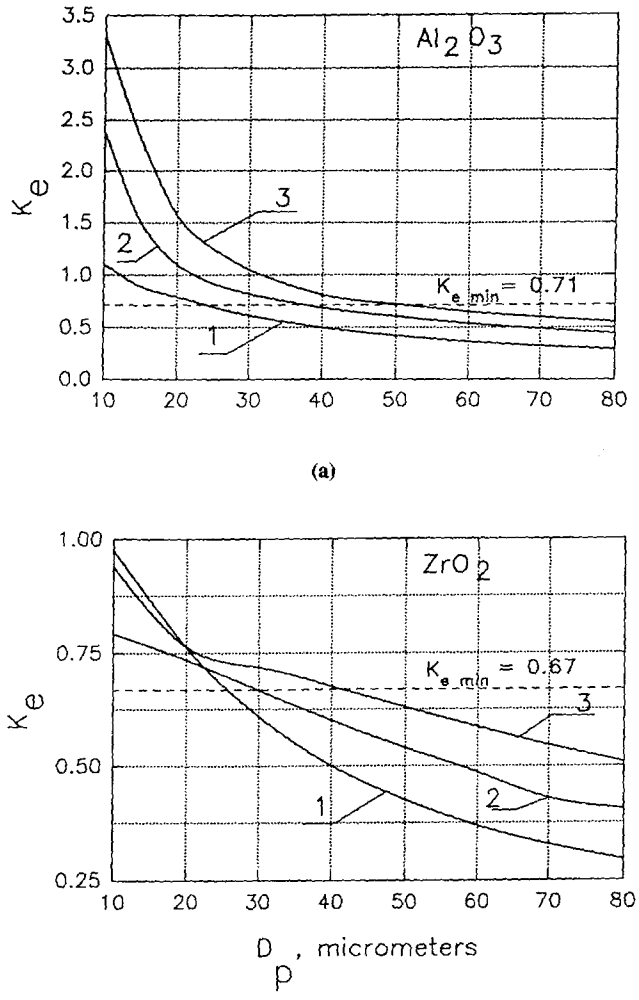

Fig. 7 Energy parameter K_e for (a) Al_2O_3 particles and (b) ZrO_2 particles as a function of particle size for gas dynamical path configurations 1 to 3. $K_{e\,min}$ corresponds to the attainment of the melting point by the particles; particles with $K_e < K_{e\,min}$ do not reach the melting point.

sonic and combined channels. This is explained by thermal relaxation; that is, the temperature of the small particles becomes equal to the flow temperature, and further increase in the energy parameter is possible only with increased velocity. Therefore, the use of an elongated supersonic channel is justified for this range of ZrO_2 particle size. Overall, the energy parameter value during spraying of ZrO_2 is less than 1, and only for particles smaller than 10 μm does it reach 0.98 in the supersonic channel and 0.94 in the combined channel.

7. Conclusions

A numerical analysis for three different HVOF system designs was performed. The velocity and thermal state were calculated for 10 to 80 μm tungsten carbide and aluminum oxide particles at different operating parameters in an HVOF system with a supersonic accelerating channel (taking into account the thermal relaxation of the Al_2O_3 particles). A pressure increase from 0.5 to 1.5 MPa strongly affects the velocity of various size particles, increasing the velocity by about 40% for medium-size particles. At the same time, particle temperature is little affected by the pressure in the combustion chamber and is almost solely determined by particle size. The results indicate that the optimal range of pressures for the operation of a modern HVOF system is 1.0 to 1.5 MPa; further increase in pressure does not significantly enhance velocity. The effect of thermal relaxation between fine particles (smaller than 30 μm) and the gas phase manifests itself in the decrease of particle temperature with the increase of pressure in the combustion chamber. Temperature in the combustion chamber affects both velocity and temperature of the sprayed particles. The velocity of the particles in all size ranges at $T_0 = 3000$ K is significantly (20 to 25%) higher than at 2000 K, whereas at 2500 and 2000 K the difference in velocities is insignificant (approximately 5 to 10%). There is a large difference between the final temperatures of metal and oxide ceramic particles due to higher specific heat and lower heat conduction of the ceramics; for example, Al_2O_3 particles larger than 20 μm

do not reach their melting point even when accelerated to high velocities (900 m/s). This can create problems during spraying and result in a lower-quality ceramic coating.

To enhance the performance of HVOF jets, in particular those used for spraying of high-melting-point materials, we propose the development of gas feed schemes with functionally separated regions of heating and acceleration, including special heating regions having low-velocity gas flow and containing subsonic and supersonic accelerating channels. Calculations of the energy parameter K_e, which incorporates both kinetic and thermal energies of a particle for such a configuration, demonstrate that this approach is correct and suggest a new family of more efficient HVOF systems. Optimization of the gas path for each particular powder is necessary to achieve maximum use of the energetic potential of the HVOF method. Powder material and particle size distribution information can be used to determine the optimal length ratio of the subsonic and supersonic channels.

The quantitative results obtained by this analysis offer a number of data for future experimental comparison and research; however, they should be used with some caution since they involve several approximations, including the quasi-one-dimensional approximation. The exact particle velocities can be calculated only if the two dimensional gas flow and the effects of cooling and friction at the barrel walls are considered. Nevertheless, the fundamental analysis of interactions in the two-phase supersonic flow should provide insight into principles of HVOF systems operation, enabling design of more efficient HVOF systems and expansion of the applicability of the HVOF method.

Acknowledgments

The authors are grateful to C. Florey for valuable comments and discussion. This work has been partially supported by the Soros Science Foundation.

References

1. M.L. Thorpe and H.J. Richter, A Pragmatic Analysis and Comparison of HVOF Processes, *J. Thermal Spray Technol.*, Vol 1 (No. 2), 1992, p 161-170
2. G.H. Smith, J.F. Pelton, and R.C. Eschenbach, Jet Plating of High Melting Point Materials, U.S. Patent, 2,861,900, 1958
3. Hobart Tafa Technologies, Inc., Technical Bulletin 1.3.2.2.4, Feb 1992
4. L. Landau and E. Lifshitz, *Fluid Mechanics*, Pergamon Press, London, 1959, p 75
5. K.M. McHugh and J.F. Key, Use of de Laval Nozzle in Spray Forming, *Thermal Spray Coatings: Research, Design and Applications*, C.C. Berndt and T. Bernecki, Ed., ASM International, 1993, p 75-79
6. J.A. Browning, Internal Burner Type Flame Spray Method and Apparatus Having Material Introduction into an Overexpanded Gas Stream, U.S. Patent 4,568,019, 1986
7. O. Knotek and U. Schnaut, Process Modeling of HVOF Thermal Spraying Systems, *Thermal Spray: International Advances in Coating Technology*, C.C. Berndt, Ed., ASM International, 1992, p 811-816
8. O. Knotek and U. Schnaut, Numerical Simulation of the Influence of HVOF Spraying Parameters on Coating Properties, *Thermal Spray Coatings: Research, Design and Applications*, C.C. Berndt, Ed., ASM International, 1993, p 7-12
9. A.V. Liykov, *Theory of Heat Conduction* (in Russian), Nauka, Moscow, 1967, p 600
10. R.I. Nigmatulin, *Dynamics of Many-Phase Media* (in Russian), Nauka, Moscow, 1987, p 464
11. Y.M. Lee and R.A. Berry, Quasi-One-Dimensional Analysis of the Two-Phase Flow in a de Laval Spray Coating Nozzle and Exit Plume, *Thermal Spray Coatings: Research, Design and Applications*, C.C. Berndt, Ed., ASM International, 1993, p 67-74
12. U.G. Pirumov and G.S. Roslyakov, *Gas Dynamics of Nozzles* (in Russian), Vol 1, Nauka, Moscow, 1990, p 364
13. V.A. Kot, Thermal Conditions of Metallic Gas Coating Formation (in Russian), *News Belarus Acad. Sci.*, 1982, p 114
14. A. Shapiro, *Dynamics and Thermodynamics of Compressible Fluid Flow*, Vol I, Ronald Press, 1953, p 78-83
15. R. Gourant and K. Friedrich, *Supersonic Flows and Shock Waves*, Interscience, 1953